Available online at www.sciencedirect.com
ScienceDirect
Chemical Physics 338 (2007) 237–251
Chemical Physics
www.elsevier.com/locate/chemphys

Dipole mediated tunnelling: Robust single-pulse population transfer across dipolar double-well systems

Avijit Datta [1], Christoph A. Marx [2], Christoph Uiberacker [3], Werner Jakubetz *

Institut für Theoretische Chemie, Universität Wien, Währinger Straße 17, 1090 Wien, Austria

Received 17 January 2007; accepted 23 March 2007
Available online 28 March 2007

Abstract

Single pulse dipole mediated tunnelling at frequencies tuned approximately to the vicinity of the direct 1-photon and multiphoton tunnel transitions is explored as a mechanism of population transfer across asymmetric dipolar 3-level lambda- (K-) or N-level extended K-systems. These systems may be purely sequentially coupled, with zero dipole matrix coupling elements for non-neighbouring states along the legs of the K. In simulations for model systems with typical molecular parameters, dipole mediated tunnelling is found to be a highly efficient strong-field mechanism of population transfer with remarkable robustness properties, in particular so for higher-order multiphoton processes.

Keywords: Population transfer; Dipole moment; Driven tunnelling; Isomerisation

1. Introduction

In this paper, we describe single-pulse state specific population transfer across lambda- (K-) or extended K-systems. This type of population transfer, which is mediated by a difference of the permanent dipole moments of the initial and target states, corresponds to direct spectroscopic transitions between two states separated by a barrier, representing a case of driven quantum tunnelling [1]. It is driven as a single- or multiphoton transition by generalised p- or multiple-p-pulses [2,3] and proceeds in a Rabi-type dynamics [1,4,5]. The presence of the dipole moment differences is sufficient to drive the transitions in otherwise purely sequentially coupled K- and extended K-systems (with zero dipole matrix elements for all tunnelling and overtone transitions), where its effects can be studied "in isolation". The mechanism may thus be characterised as dipole-mediated tunnelling (DMT). Much less pronounced and less robust effects are obtained for non-polar systems upon inclusion of direct overtone couplings into the dipole matrix, and, quite obviously, by the inclusion of tunnel couplings.

The effects of dipole moment differences on laser-driven transfer processes have been studied extensively by Meath and co-workers, with a wealth of information obtained in particular for 2- and 3-level systems [6–8]. An important consequence of non-zero dipole moments is the feasibility of multiphoton processes that are forbidden in non-polar systems [6]. Even more importantly, their results, obtained within various different approximations and formalisms, e.g. within (and extending) the rotating wave approximation [5,9], also show that under quasiresonant conditions non-zero dipole moments induce additional overtone processes, where, however, in order for such dipole induced processes to become effective usually a direct non-zero dipole matrix coupling must also be present. Note that in

* Corresponding author. Tel.: + 43 1 4277 52758; fax: + 43 1 4277 9527.
E-mail address: werner.jakubetz@univie.ac.at (W. Jakubetz).
[1] Present address: Shibpur Dinobundhoo Institution, Howrah 711 102, India.
[2] Present address: Department of Chemistry, University of California, Irvine, CA 92697, United States.
[3] Present address: Austrian Research Centers GmbH, 2444 Seibersdorf, Austria.

0301-0104/$ - see front matter © 2007 Elsevier B.V. All rights reserved.
doi:10.1016/j.chemphys.2007.03.017

K- or extended K-systems such overtone processes may represent tunnelling transitions. Previously two of us [10] have found in an investigation of stimulated Raman adiabatic passage (STIRAP) [11–14] in polar systems, that such dipole-related effects extend to off-resonance conditions, where they can become extremely pronounced.

Population transfer across (extended) K-systems may be considered to describe molecular isomerisation processes proceeding in double-well potentials [15,16]. Robust methods of population transfer are quite essential in this context in view of possible disorder of the reagents. Given the highly specific properties of usual p-pulse transitions [5], standard two-pulse pump–dump-type methods of driving molecular isomerisation can be adversely affected even by the fairly low degree of disorder that would occur for oriented reagent molecules. In contrast to such techniques, DMT can show remarkable robustness, particularly so for multiphoton transitions. The effects are large enough to allow an implementation accounting for orientational disorder.

Furthermore, the transfer dynamics of DMT largely avoids transitional population of the apex state. Thus with respect to the phenomenology of DMT there is a remarkable analogy to the STIRAP technique, which for pure (i.e. sequentially coupled non-polar) K-systems is well known to give rise to robust population transfer without involvement of the apex state. Interestingly, at least for the model systems investigated, it also turns out that the two techniques require similar field amplitudes and pulse lengths – where, however, only one pulse is required in DMT.

In this communication, we report simulations for a number of model systems of small to moderate complexity, starting off from 3-level K-systems with various degrees of asymmetry. The paper is organised as follows: in Section 2, we provide a description of the model 3-, 5-, and 11-level systems used in the investigations. We specify our system parameterisations, in particular the different pump-to-dump ratios, i.e. the ratios between the level spacings on the two legs of the K that characterize the asymmetry of the systems, and we also describe the technical aspects of our simulations. In Section 3, we present our simulations of population transfer in asymmetric 3-level K-systems driven by a single Gaussian laser pulse. In these simulations, we cover an extended range of pulse amplitudes, and wavelengths well into the far-infrared range in order to also deal with higher order multiphoton transitions. We investigate separately the effects of dipole moment and tunnel coupling dipole matrix elements in comparison with a simple sequential K-system. In Section 4, we extend these investigations to 1 + 1, 1 + 2, 2 + 1 and 2 + 2 quantum transfer in 5-level extended K-systems, again considering different pump-to-dump ratios, and investigating now also separately and explicitly the effects of overtone coupling elements. Here, as throughout the paper, in order to unequivocally characterize any state-specific transition we use the notation "m + n quantum transfer" in terms of pump- and dump-quanta in sequentially coupled non-polar systems; note, however, that for DMT this nomenclature does not reflect the physical nature of the processes in terms of their photonicities. In Section 5, we deal with an 11-level system representing parts of the HCN- and HNC-bend progressions, thus providing a very simplistic reduced basis set model of HCN ! HNC isomerisation with bend pre-excited reagent molecules. Finally, a summary of our results and our conclusions is given in Section 6.

2. Model systems

2.1. Three- and five-level systems

With molecular applications in mind, we use a number of model systems parameterised with values loosely adapted from the HCN/HNC system (see Section 2.2). In this way, our investigations also connect to our previous studies [10,17] of population transfer in extended K-systems by the STIRAP (stimulated Raman adiabatic passage) technique, as well as to several other related investigations [16,18,19]. Clearly, upon rewriting the parameters in terms of dimensionless reduced variables, our results should also scale to different energy or frequency regimes. For convenience with the resulting numerical values we also make use of atomic units (a.u.) with the following conversion factors: 1 a.u. of field strength = 5.14225 GV cm^{-1}, 1 a.u. of energy = 1 hartree = $4.35981 \cdot 10^{-18}$ J, 1 a.u. of dipole moment = 2.54176 D = $8.47841 \cdot 10^{-30}$ C m.

Fig. 1 illustrates the model systems. Since the 5-level systems are direct extensions of the 3-level system, both are shown in the same graph. Our basic unit is a sequentially coupled asymmetric 3-level K-system, where the two lower levels, denoted, respectively, R1 and P1, assume the roles of the "initial" (or reagent) state and the "target" (or product) state, while the "apex" state (A) corresponds to the transition state. The notation is chosen in view of the necessary extension to the 5-level system. We fix the energies of P1 and A (with difference De = 0.0034 a.u.) while allowing R1 to vary, so that the zero-order pump- and dump frequencies, and accordingly also the zero-order R1 ! P1 transition frequencies, can assume different ratios. Covering pump-to-dump ratios in the range from nearly symmetric (≈1:1) to strongly asymmetric (≈2:1), and avoiding the two very special limiting cases, we use the values 21:17, 4:3, 3:2 and 30:17. Note the HCN/HNC system has a pump-to-dump ratio close to 3:2 [10,17]. The main purpose of this variation is the investigation of the role of the apex state as a rung in level climbing from the initial to the target state. For simply commensurate ratios of the pump- and dump-frequencies, the apex state could act as an exact rung in low-order multiphoton transitions, which may enhance population transfer.

Fig. 1 displays the 3- and 5-level systems for the specific pump-to-dump ratio of 4:3, and also shows the values of

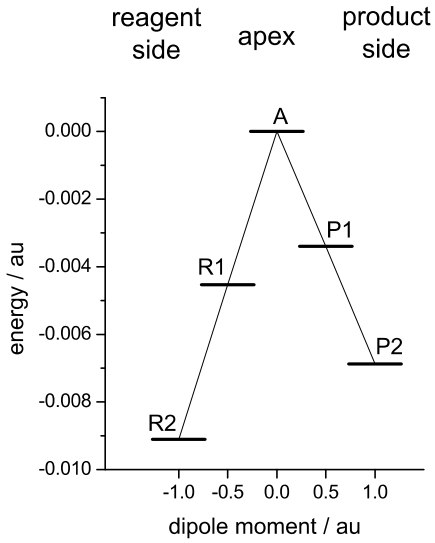

Fig. 1. Energy level and dipole moment scheme of the model 3-level and 5-level systems. The 3-level systems do not include the states denoted R2 and P2. The plot shows the systems denoted "dipolar" for a pump-to-dump ratio of 4:3. Other ratios are obtained by shifting the levels R1 and R2. Only sequential dipole matrix coupling elements as indicated by thin lines are non-zero, all remaining non-diagonal elements are set to zero. The systems denoted "sequential" have zero dipole moment for all levels; the systems denoted "tunnel couplings" and "overtone couplings" are obtained from the non-polar sequential one by adding non-zero dipole matrix elements as shown in Table 1.

the dipole moments for the individual levels. The values of the non-diagonal dipole matrix elements used in all 3- and 5-level model systems are given in Table 1. In the basic model, denoted "sequential", i.e. the standard sequentially coupled non-polar 3-level K-system, all diagonal elements and the P1–P2 coupling element of the dipole matrix are zero. In the "sequential dipolar" model, which is the one giving rise to the DMT mechanism in isolation, we have non-zero diagonal dipole matrix elements. We also investigate separately tunnelling transitions in the non-polar system mediated by a non-zero R1–P1 dipole matrix element, for which we use the notation "tunnel coupling". Finally, the case of a fully coupled dipolar system is denoted "full". In the full system, different tunnelling mechanisms may be present, with the possibility of constructive or destructive interference.

Table 1
Dipole matrix coupling elements in the 3- and 5-level model systems

Type of coupling	Coupled levels[a]	Dipole matrix element[b]
Sequential	R1–A, P1–A	0.20
Sequential	R2–R1, P2–P1	0.25
Tunnel	R1–P1	0.02
Tunnel	R1–P2, R2–P1	0.005
Tunnel	R2–P2	0.002
Overtone	R2–A	0.05
Overtone	P2–A	0.05

[a] For the notation, see Fig. 1.
[b] In atomic units.

From the 3-level systems we derive extended-K 5-level systems by adding the levels R2 (on the reagent side) and P2 (on the product side), in such a way that both progressions show a moderate degree of anharmonicity, with values adapted from the HCN/HNC system. In detail, the A–P2 energy difference is set to 2De + 0.0008 a.u., while the reagent ladder spacing is obtained by suitable linear scaling of 2De + 0.0004 a.u. As an additional coupling mechanism, non-zero overtone coupling elements R2–A and P2–A may be present in the dipole matrix ("overtone coupling"). Again we will also consider tunnel coupling as well as the fully coupled dipolar systems.

2.2. A simplistic 11-level model system for HCN ! HNC isomerisation

The energy levels [20] and dipole matrix elements [21,22] for our 11-level extended K-system are taken from ab initio calculations and a J = 0 model of the HCN/HNC molecular system [20]. We have previously used the full 550-level system as well as various differently truncated versions in a number of contexts from optimal control and STIRAP to background state control (see, e.g. Refs. [10,17,21,22] and articles quoted there). For the present purpose we use the 10 energetically highest localised states of the HCN and HNC bend progressions, i.e. the four even J = 0 HCN states from $(v_1, v_2, v_3) = (0, 16, 0)$ to $(0, 22, 0)$, and the six even J = 0 HNC states from $(0, 12, 0)$ to $(0, 22, 0)$, together with a delocalised apex state joining the two progressions (the transition state). In this model, in the full calculations all dipole matrix couplings are present, so that there are no zeroes in the dipole matrix, but in order to analyse the results, we will also apply modified systems with various dipole matrix elements set to zero.

The full 11-level system may be considered to provide a simplistic reduced basis set model describing isomerisation of a highly bend-pre-excited HCN molecule. In the simulations reported below, the HCN state $(0, 18, 0)$ is used as the initial state. There are two stringent approximations beyond the reduced-basis set assumption. The first one is the neglect of the split nature of the transition state [17] (see also Ref. [19]). In a zero order picture of the HCN/HNC bend levels, the transition state originates from plus- and minus combinations of the near-degenerate HCN and HNC bend states $(0, 23, 0)$ [20], and thus includes two delocalised levels with different symmetry properties. We will briefly return to this point in Section 5. The second important approximation is the neglect of molecular rotation. While this may be of little concern in the consideration of formal N-level systems, it can be important in molecular applications, where rotational motion will be pronounced on a picosecond time scale [23,24].

2.3. Laser fields

All calculations in the following sections are carried out for laser pulses with Gaussian envelope and fixed pulse

duration (full width at half height) of 7.2 ps in the field strength, corresponding to a width of 5.1 ps in laser intensity. The only parameters we vary are the peak field amplitude A_0 and the wavelength k. We consider values of A_0 in the range from 0 to 0.009 a.u. (460 MV cm^{-1}) for the 3- and 5-level systems, and up to 0.02 a.u. (1 GV cm^{-1}) for the HCN/HNC model systems. These values correspond to laser intensities of 2.8 and 13.9 TW cm^{-2}, respectively, and are well below the Keldysh ionisation limit [25,26] of about 0.024 a.u. = 20 TW cm^{-2}. For k we cover the range from about 3 to 130 l m, corresponding to wave numbers from about 3000 down to 75 cm^{-1}. This range is chosen to include at least the direct 2-photon process from the initial state to the target state for all our systems, and where possible higher order photonicities, which provide favourable conditions for DMT.

We also note that the choice of the pulse parameters is partially motivated by the fact that STIRAP population transfer in similar model systems requires laser fields with comparable parameters [10,17]. The results of the present paper should thus indicate to what extent DMT could be considered a viable alternative to STIRAP in molecular population transfer processes.

2.4. Computational techniques

In our simulations, the time-dependent Schrödinger equation describing the interaction of the driving laser field with the model systems, which are assumed to be aligned with respect to the linearly polarised fields, is integrated numerically using a fourth-order Runge–Kutta method. The use of 200 integration steps per optical cycle was found to give rise to fully converged results.

3. Population transfer across dipolar K-systems

3.1. Gross features

We start by considering the threshold excitation patterns, showing how at low field strengths the resonant p-pulses emerge close to the zero-order wavelengths. Note we use the wavelength as independent variable in order to stress the progression of the n-photon processes, where the zero-order resonance wavelengths scale linearly with n. Fig. 2 shows the k-dependence of the R1 ! P1 transition probability at $A_0 = 0.002$ a.u. for the different pump-to-dump ratios. The excitation patterns for the (non-polar) sequential systems in the upper panels illustrate the selection rules valid for the dipole-free case [7,27,28]: only even n-photon direct excitation is allowed for a process with an even overall number of quantum steps, here the two-quantum transition R1 ! A ! P1. This means that the transition near the nominal R1 ! P1 resonance is absent from the excitation spectrum. The 2-photon process is well developed, while all even higher order transitions are still below threshold and require stronger fields. In contrast

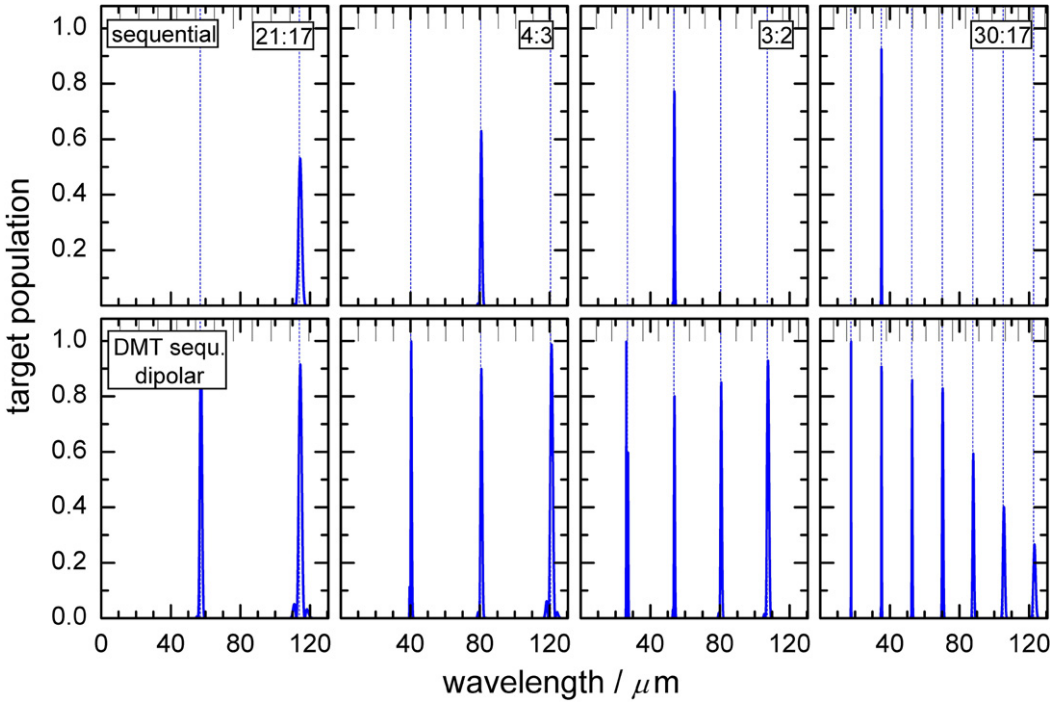

Fig. 2. Low-field excitation spectra for single-pulse R1 ! P1 population transfer in 3-level K-systems for a laser pulse peak amplitude $A_0 = 0.002$ a.u. Top row panels are for the non-polar sequential systems, bottom row panels for DMT in the dipolar systems. Pump-to-dump ratios for each column are identified in the respective top panels. Thin broken lines (online blue) mark the zero-order wavelengths for successive direct n-photon transitions; grey vertical lines near the upper borders denote zero-order wavelengths for successive n-photon pump transitions R1 ! A. The plots show the emergence of resonant p-pulse excitation. (For interpretation of the references to colour in this figure legend, the reader is referred to the web version of this article.)

the complete progression of direct n-photon transitions is present for the dipolar, but purely sequentially coupled systems, as shown in the bottom panels of Fig. 2.

For the dipole-free case, the efficiency of population transfer drops along the sequence 30:17 towards 21:17, which appears to be related to the availability of the apex state as a rung state (compare the detunings and orders of the n-photon pump transitions shown along the upper borders of the plots). No such considerations seem to be of concern for the dipolar systems, where all transitions, including high-order ones, are well developed at $A_0 = 0.002$ a.u.

The low-field range is the realm of analytical models and low-order perturbation theory, from which a number of results have been derived for single- and multiphoton population transfer in dipolar systems [6–8,27,28]. Nevertheless, a more detailed look at the results of the full numerical simulations may be useful. Whereas the peak patterns can be predicted from analytical models, the differences arising in the transitions to the target and apex states in the possible coupling schemes of a 3-level system, and in particular possible interference contributions between different pathways are not readily obtained from the perturbation series.

Fig. 3 collects results for the 30:17 system, for which we expect only weak perturbations from competing multiphoton transfer through the apex state (contrary to the simply commensurable cases 3:2 and 4:3, for which such effects occur, as will be shown in Section 3.2). For the sequentially coupled non-polar 3-level system, with the diagonal dipole matrix elements and the R1–P1 coupling element all zero, the n-photon transitions with odd n are absent, while for even n only the lowest (i.e. 2-photon-) peak is present and all higher order transitions are still below threshold. Conversely, only odd-photonicity transitions to the apex-state are allowed. At $A_0 = 0.002$ a.u. the 1- and 3-photon transitions are present, and are very weak.

Adding tunnel coupling to the non-polar system renders all multiphoton transitions to A and P1 allowed; in particular the 1-photon transition to P1 and the 2-photon transition to A are fully developed at $A_0 = 0.02$ a.u., whereas all higher order transitions are still below threshold. In fact the peak seen near 17.5 l m represents the 5p-pulse for 1-photon R1 ! P1 transfer; for the 7.2 ps Gaussian fields the p-pulse has $A_0 = 0.00050$ a.u. at a resonance wavelength $k_r = 17.5353$ l m, weakly red-shifted from the zero order value 17.5243 l m. Alternatively, the dipolar system with zero R1–P1 tunnelling matrix element shows the very pronounced effect of DMT "in isolation": the whole sequence of n-photon transitions to P1 is present up to at least n = 7, and is structured in the expected way, becoming weaker with increasing n. On the other hand, the DMT p-pulse transition requires a 4 times stronger field than in the simple tunnel case, with field parameters $A_0 =$

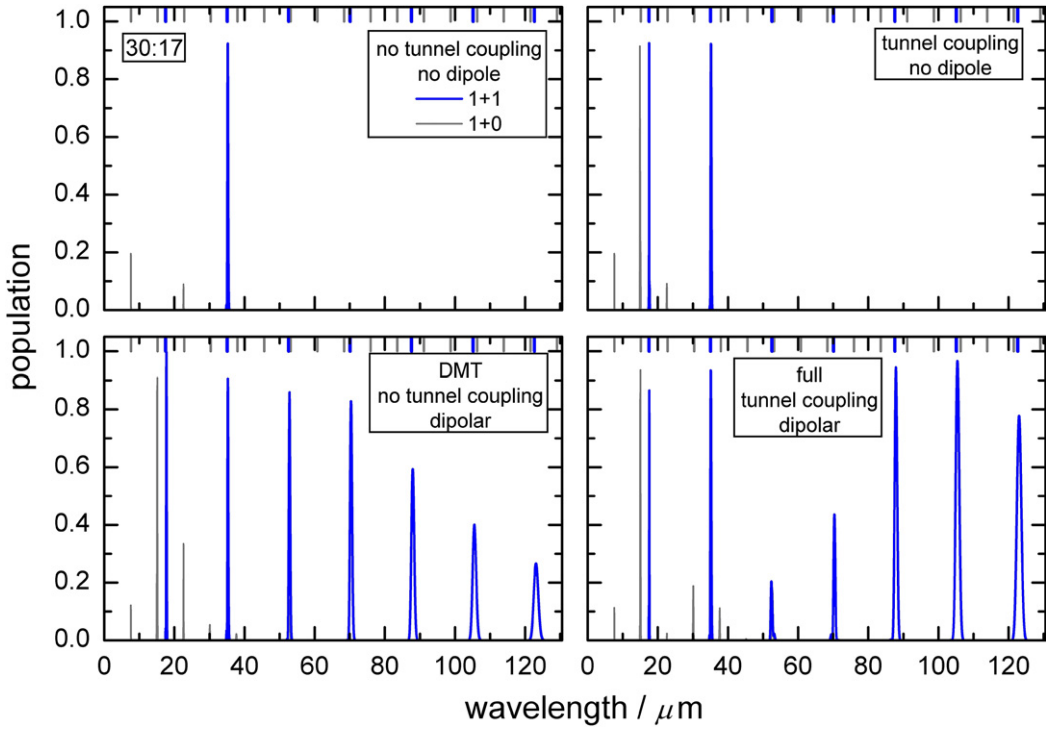

Fig. 3. Detailed low-field excitation spectra for single-pulse R1 ! P1 population transfer in 30:17 3-level K-systems for a laser pulse peak amplitude $A_0 = 0.002$ a.u., for coupling schemes and dipole conditions as indicted in each panel. Bold lines (online blue): target state (P1) populations; thin grey lines: apex state (A) populations. Bold marks (online blue) and grey marks at upper border denote sequential n-photon zero order transition wavelengths for R1 ! P1 and for R1 ! A transitions, respectively. (For interpretation of the references to colour in this figure legend, the reader is referred to the web version of this article.)

0.001974 a.u. and $k_r = 17.6983$ l m, considerably red-shifted. The peak seen in Fig. 3 thus represents the p-pulse. Clearly already close to threshold DMT behaves differently from standard tunnelling in quantitative terms. Note that in contrast the effect on the P1–A transition is not pronounced and is comparable with the situation in the non-polar tunnelling-coupled case, due in part to the fact that the dipole moment difference is only half the one between the R1 and P1 states. Finally, in the fully coupled dipolar system the presence of the direct tunnel coupling weakly modifies the features observed for pure DMT, although it does not give rise to any qualitative changes. This is an important result, as in a realistic system the fully coupled case, and not the somewhat artificial pure DMT situation will be the rule. Again there is only a weak effect on the R1–A transition. Note also that at this comparatively low field strength the transitions still have the expected sharp resonance-like appearance; the remarkable robustness of the transitions announced in the Introduction arises only for distinctly higher field strengths.

Switching now to such stronger fields, Figs. 4 and 5 illustrate the case $A_0 = 0.0065$ a.u. for the 4:3 and 3:2 systems, respectively. For the sequential systems, the increase in laser intensity by a factor 10 compared to the situation in Figs. 2 and 3 causes only slight changes in the excitation patterns. The 2-photon resonance peaks broaden slightly, the Bloch–Siegert shifts [29] displacing the bands away from the zero-order resonance frequencies increase slightly, and the 4-photon peak is seen to emerge for the 3:2 system. In marked contrast, for DMT in the dipolar systems we observe a huge increase in "reactivity", signalled by a massive broadening of the resonance ranges. Note also that here the Bloch–Siegert shifts are sizable.

In comparison, the inclusion of direct tunnel coupling leaves a much more specific standard resonance pattern

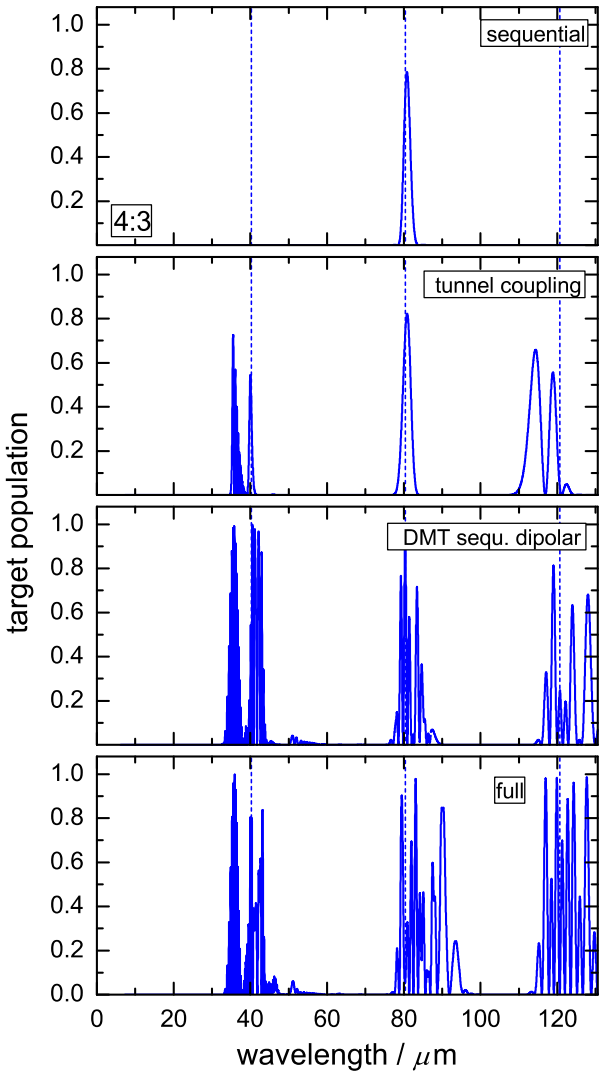

Fig. 4. Excitation spectra for single-pulse R1 ! P1 population transfer in 4:3 K-systems at higher field strength ($A_0 = 0.0065$ a.u.). From top to bottom the panels show in turn the results for the non-polar sequential system, the non-polar system with added tunnel matrix elements, the dipolar sequential system with pure DMT transfer, and the fully coupled dipolar system. Plot conventions are as in Fig. 2.

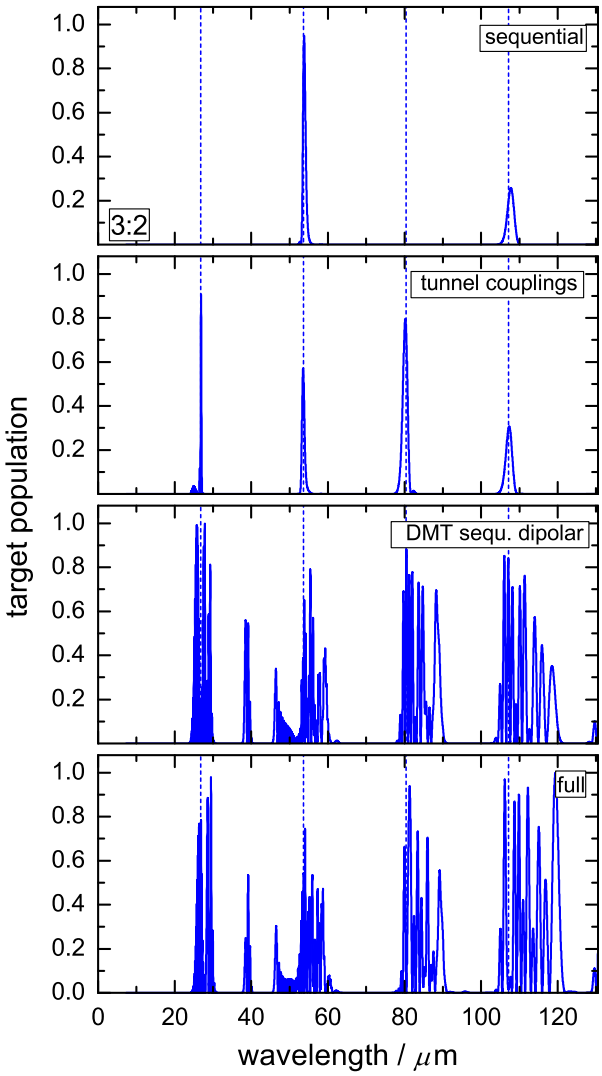

Fig. 5. Excitation spectra for single-pulse R1 ! P1 population transfer in 3:2 K-systems. All other properties and plot details as in Fig. 4.

for the population transfer. In the fully coupled systems (bottom panels of Figs. 4 and 5), as noted in the discussion of Fig. 3, interactions between the two different tunnelling mechanisms may be expected. In view of the rather small magnitude of the effect induced by matrix coupling these interactions should be not too significant. Indeed, comparison of the pure DMT mechanism in the sequentially coupled system with the results from the fully coupled dipolar system shows only minor differences between the two cases.

The full extent of the broad structures observed for DMT can be studied in more detail by considering the simultaneous variation of A_0 and k. Fig. 6 collects a series of contour plots in the (A_0, k) plane for the sequentially coupled dipolar systems. In each of the panels we zoom into a wavelength range corresponding to one of the extended features in the vicinity of the n-photon thresholds for direct R1 ! P1 transitions. In a number of cases, we observe several connected progressions of multiple p-

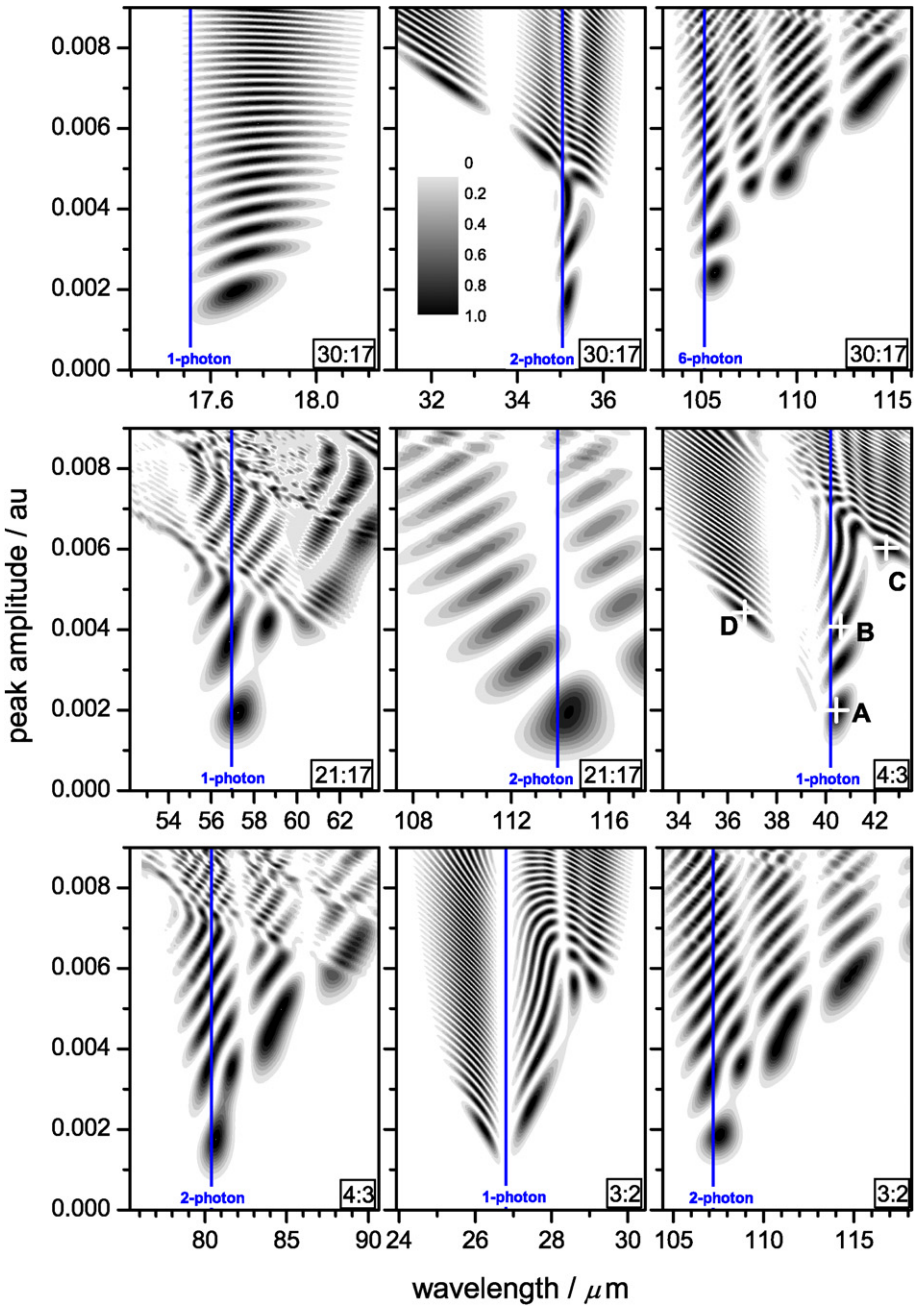

Fig. 6. Contour plots in the (k, A_0) plane for DMT single pulse R1 ! P1 population transfer in sequentially coupled dipolar K-systems with pump-to-dump ratios as identified in each panel. Vertical lines (online blue) denote zero-order n-photon transition wave-lengths as indicated. Points A–D in the middle right panel denote pulse conditions, for which the population dynamics are shown in Fig. 7. The individual plots zoom into ranges, where for suitably chosen pulse parameters robust population transfer may be expected even in partially disordered samples. (For interpretation of the references to colour in this figure legend, the reader is referred to the web version of this article.)

pulses, a feature to be addressed in Section 3.2. Furthermore, each of the individual resonance peaks is remarkably extended, so that consecutive multiple-p pulses are rather densely spaced along both coordinates. This suggests considerable overall robustness of the population transfer, and in particular it will allow a pulse setup that can cope with orientational disorder. Selecting a pulse with high field strength at suitable wavelength, the projections even onto systems that are substantially de-aligned with the field vector would still induce significant population transfer.

3.2. Specific features: effects of the detailed level structure

The contour plots in Fig. 6, as well as the conspicuous doubling of the 1-photon peak strongly apparent in Fig. 4 for the 4:3 case, and, less discernible, also in Fig. 5 for the 3:2 case, show that in addition to the usual np-pulse progressions there can be further mechanisms inducing population transfer. In Fig. 7, we demonstrate this fact for the 4:3 system near the 1-photon R1 ! P1 transition. We show the population dynamics for pulses with parameters marked A–D in the middle right panel of Fig. 6, which give rise to several local maxima in the transition probability. At points A and B the Rabi-like dynamics of a resonant p-pulse (field A) and a 5p-pulse (field B) are clearly apparent from the population dynamics. There is only little transitional apex state population. Adiabatic Floquet analysis [3,9,30–32] performed for these pulses shows avoided crossing structures in the quasienergy correlation diagrams, caused by the interaction of the two quasienergy states that asymptotically correspond to the initial and the target state, and do nowhere pick up contributions from the third (apex) state. Consequently, there is little apex participation in the population dynamics. In contrast, at points C and D we find avoided crossing patterns between quasienergy states in which all three asymptotic levels participate significantly. Hence, both at point C and point D we observe massively perturbed Rabi-dynamics and pronounced transitional apex state population. In detail, case C corresponds to a perturbed p-pulse transition, and point D corresponds to a perturbed 3p-pulse. While C is the origin of a complete, but perturbed np-progression, the mechanism for the progression originating in D requires stronger fields. In any case, in the entire (A_0, k)-range the dipole moment difference gives rise to strong coupling of the three states, thus leading to the rich structure in the contour plots in Fig. 6.

An interpretation of the additional mechanism can be obtained on the basis of the commensurability properties of the 3:2 and 4:3 systems. In both cases, the 1-photon transition frequency R1 ! P1 is identical to suitable simple multiphoton transition frequencies R1 ! A and A ! P1, allowing for a multiphoton pump–dump transition driven by a single pulse. The high photonicities of the overall tran-

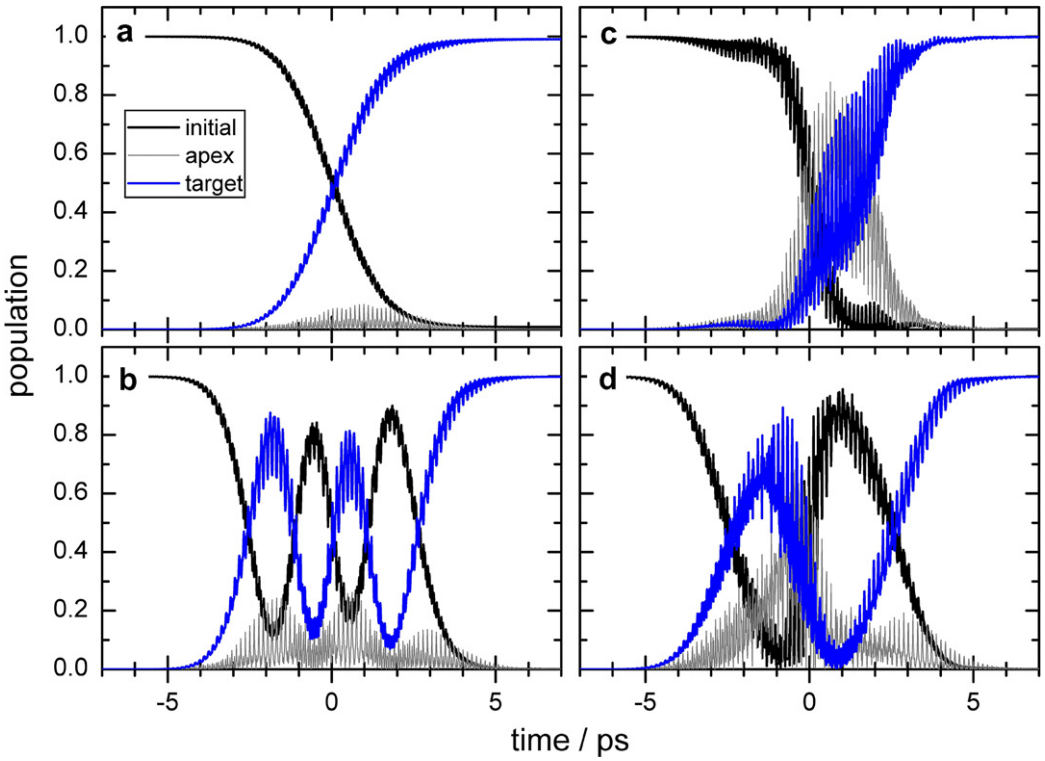

Fig. 7. DMT population dynamics in the sequentially coupled dipolar 4:3 K-system. The pulse conditions for the driving laser fields marked A–D are identified in the middle right panel of Fig. 6. Bold lines starting at abscissa value 1 (online black): initial state (R1) populations; bold lines starting at abscissa value 0 (online blue): target state (P1) populations; thin grey lines: apex state (A) populations. (For interpretation of the references to colour in this figure legend, the reader is referred to the web version of this article.)

sitions (5- and 7-photon, respectively) make these processes more demanding than 1-photon DMT transfer, so that they appear at higher field amplitudes and in strongly Bloch–Siegert shifted positions. Furthermore, at lower field strengths their appearance is heralded by distinct apex population, with increasing field strength these 3- or 4-photon processes are gradually superseded by the composite higher photonicity transitions. We note that an analogous interpretation applies to the appearance of a double-peak structure for the non-polar tunnel-coupled 4:3 system, which is clearly apparent in the plot in Fig. 4.

Multiphoton pump–dump transfer is also participating in the "additional" peaks near k = 40 l m apparent in Fig. 5 for transfer in the dipolar 3:2 system. This wavelength falls in the range in between the direct 1- and 2-photon DMT transfer. The emergence of this mechanism can be inferred from the quasienergy correlation diagrams in Fig. 8. For the non-polar system the quasienergy state correlating asymptotically with R1 does not interact sufficiently strongly with one of the other states to allow significant population transfer. The narrowly avoided crossings between the two other quasienergy states, which thus remain unpopulated throughout, are without consequences.

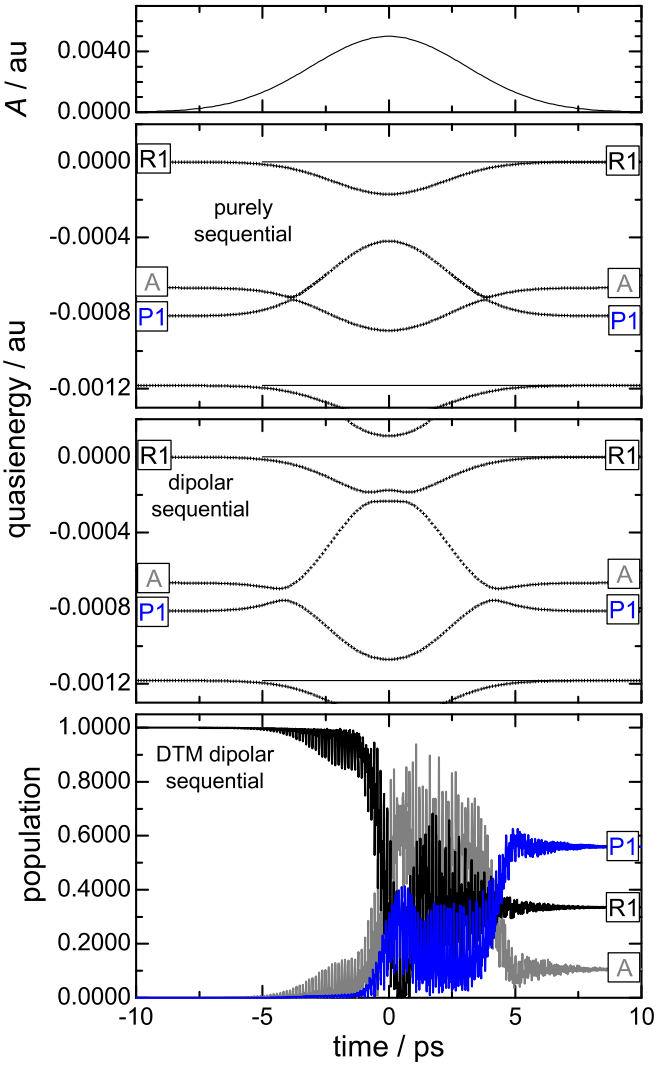

Fig. 8. Adiabatic quasienergy correlation diagrams relating to the peak near 38.51 l m for the sequentially coupled dipolar 3:2 3-level system (panel DMT in Fig. 5). The panels show in turn the field strength envelope A(t) of the Gaussian pulse with carrier wavelength 38.51 l m, the principal sheet of the quasienergy correlation diagram for the purely sequential system, the same diagram for the sequential dipolar system, and the DMT population dynamics for the sequential dipolar system. In the quasienergy plots, continuations to neighbouring sheets are included, and the asymptotic assignment of the quasienergy states is indicated by inserts.

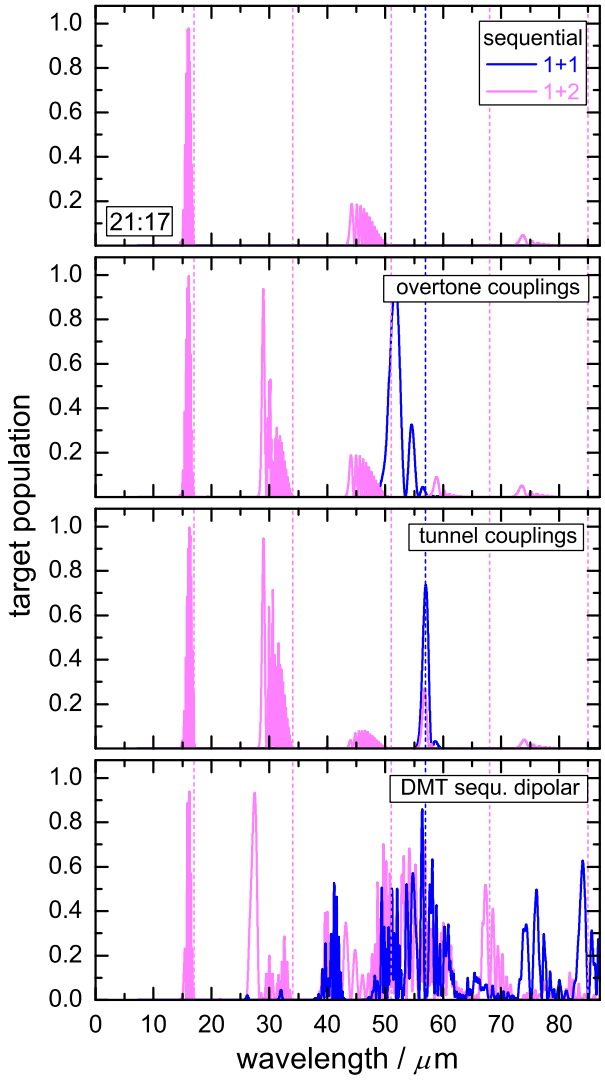

Fig. 9. Excitation spectra for single-pulse 1 + n population transfer R1 ! P1 and R1 ! P2 in 21:17 5-level extended K-systems for a peak field strength A_0 = 0.0065 a.u. From top to bottom the panels show in turn the results for the non-polar sequential system, the non-polar system with added overtone matrix elements, the non-polar system with added tunnel matrix elements, and the dipolar sequential system. Dark lines (online blue): transitions to P1, light lines (online magenta): transitions to P2. Vertical broken lines in the same colours denote zero-order n-photon transition wavelengths falling into the range. (For interpretation of the references to colour in this figure legend, the reader is referred to the web version of this article.)

The inclusion of the dipole moments completely changes the picture. Interactions between the quasienergy states are strongly enhanced. The narrowly avoided crossing between the A and P1-related states near □4 ps seen in the non-polar system turns into a massively avoided one, indicating strong interactions. More significant for the transfer is the appearance of a prolonged interaction involving the initial state near the peak of the pulse. Following the time evolution of the quasienergy curves, the interaction between the states correlating with A and P1 causes a strongly mixed character of these states for times t > □4 ps. Hence in the extended pseudo-crossing range around the peak of the field non-adiabatic transitions between the two quasienergy states populate both A and P1 from R1. If the area spanned by the energy gap at the avoided crossing and the time interval where it is maintained were p, we would have a generalised p-pulse [3,32], and with it complete exchange of population between the pseudo-crossing quasienergy states. In our specific example, this area is about 1.3p, and thus some population is transferred back to the initial state, as can also be seen from the population dynamics plotted in the bottom panel of Fig. 8. Finally, at the avoided crossing near 4 ps population is re-distributed between A and P1. Again the correlation of this population exchange with the avoided crossing is nicely displayed in Fig. 8.

Just as in the case of peak doubling described further above, the nature of the transition can also be deduced by studying its A_0-dependence. P1 population develops from a peak marking apex population with an onset exactly at the 4-photon R1 ! A threshold. With increasing field strength this transition is more strongly Bloch–Siegert shifted, so that finally the 3-photon A ! P1 transition starts to proceed as a consecutive step, and P1 population replaces A population.

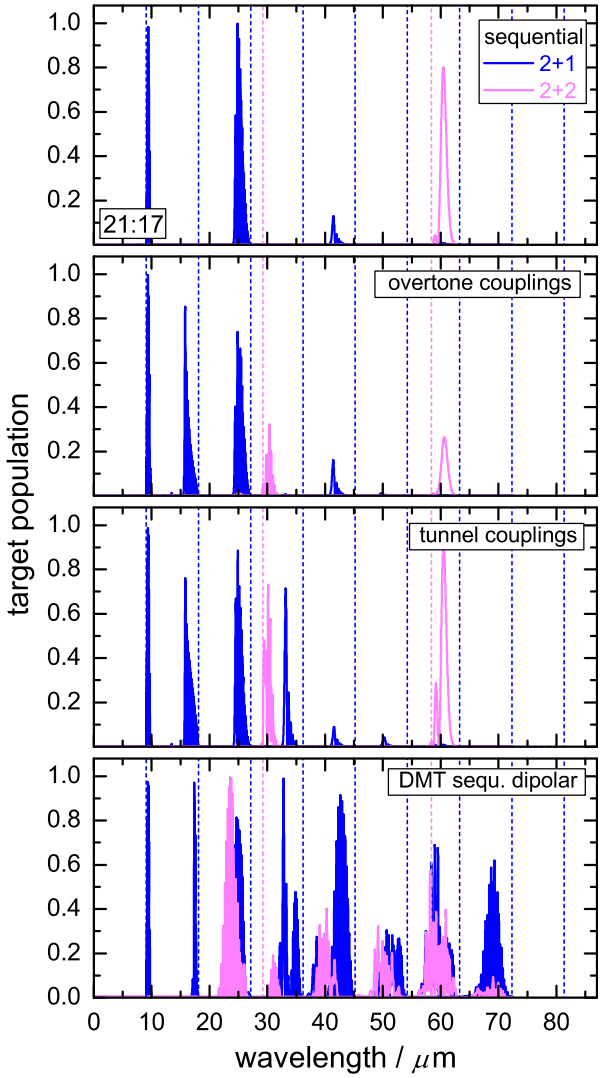

Fig. 10. Excitation spectra for single-pulse 2 + n population transfer R2 ! P1 and R2 ! P2 in 21:17 5-level extended K-systems. All other plot details and conventions as in Fig. 9.

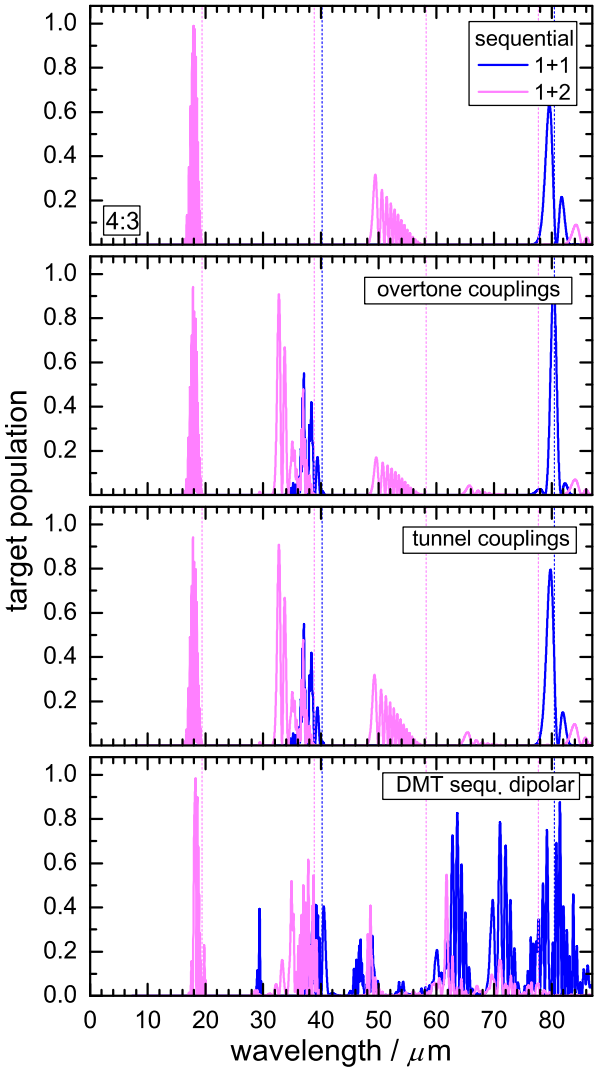

Fig. 11. Excitation spectra for single-pulse 1 + n population transfer R1 ! P1 and R1 ! P2 in 4:3 5-level extended K-systems. All other plot details and conventions as in Fig. 9.

4. Population transfer across dipolar extended K-systems

We now extend the investigations to 5-level systems. In this case, either R1 or R2 can assume the role of the initial state, and both P1 and P2 can act as target state. The various possible transfer processes can be characterised in terms of pump- and dump-quanta as 1 + 1, 1 + 2, 2 + 1 and 2 + 2 transitions. It will also be of interest to characterize the total transition probability from a given initial state to both product states.

In addition to the three mechanisms investigated for the 3-level systems, i.e. non-polar sequential, dipole matrix tunnel coupling and DMT in dipolar sequential systems, there is now also the possibility of tunnelling induced by (non-tunnelling) overtone coupling. In the dipole matrix this means the presence of non-zero direct overtone coupling elements (R1–A and P1–A). For dipole matrix tunnel coupling there are now four non-zero elements (R1 and R2 to P1 and P2).

We start by discussing some typical examples for the moderately strong field case $A_0 = 0.0065$ a.u. Figs. 9 and 10 show, respectively, the situation for 1 + n and 2 + n transitions in the 5-level system with pump-to dump ratio 21:17. Again selection rules operate for the non-polar sequential system, which demand even n-photon transitions for the even number of quantum-steps in the 1 + 1 transition R1 ! P1 (in analogy to the 3-level system) and the 2 + 2 transition R2 ! P2, but odd n-photon transitions for the 1 + 2 process R1 ! P2 and its 2 + 1 counterpart R2 ! P1, with their odd number of quantum states. Both

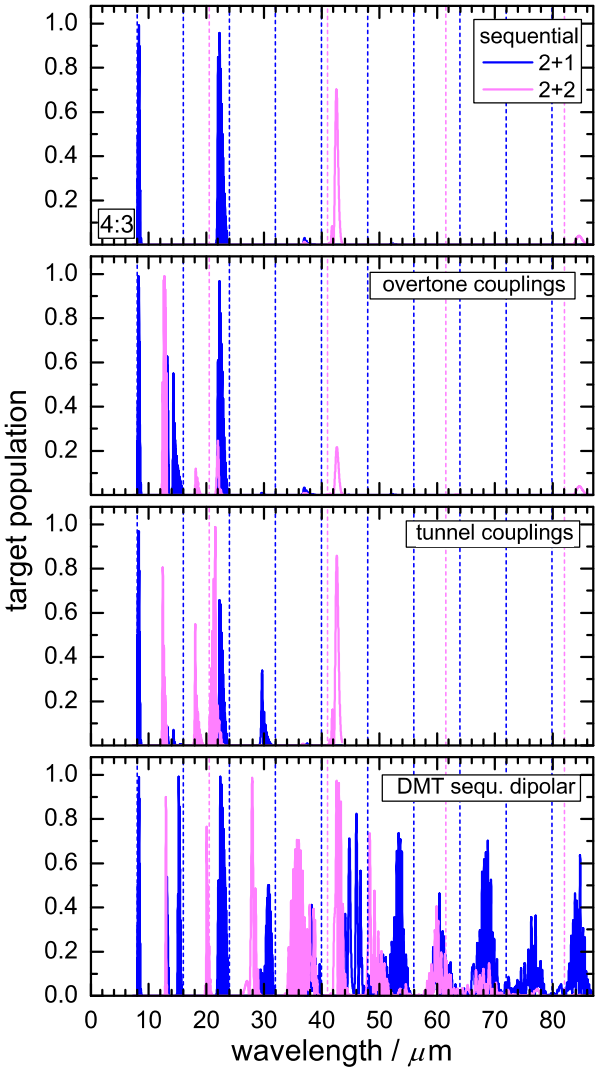

Fig. 12. Excitation spectra for single-pulse 2 + n population transfer R2 ! P1 and R2 ! P2 in 4:3 5-level extended K-systems. All other plot details and conventions as in Fig. 9.

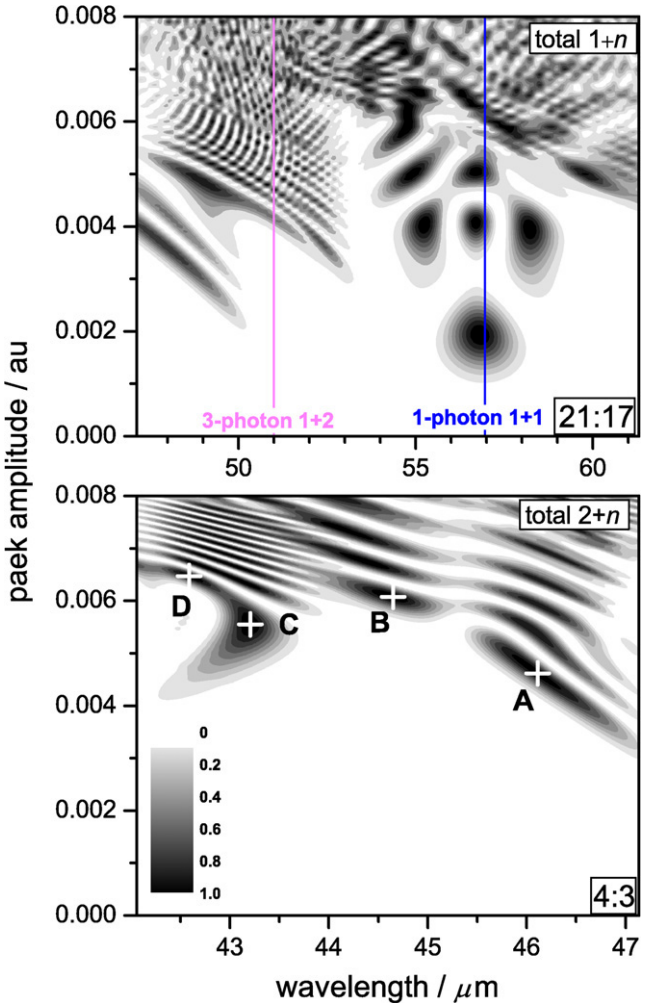

Fig. 13. Selected (k, A_0)-contour plots for DMT single pulse population transfer in dipolar sequentially coupled 5-level extended K-systems. Upper panel: total 1 + n population transfer in the 21:17 5-level system near the zero-order 1-photon 1 + 1 transition (dark vertical line, online blue) and the zero-order 3-photon 1 + 2 transition (light vertical line, online magenta). Lower panel: total 2 + n population transfer in the 4:3 5-level system in the range between the zero-order 2-photon 2 + 2 transition at 41.00 l m and the 6-photon zero-order 2 + 1 transition at 47.94 l m. Points A–D denote pulse conditions for which the population dynamics are shown in Fig. 14. (For interpretation of the references to colour in this figure legend, the reader is referred to the web version of this article.)

overtone coupling and tunnel coupling render the remaining direct single-photon and low multiphoton transitions feasible, but again it is the dipole moment in DMT that leads to strong excitations and to broad, robust features in the population transfer, particularly so for higher-order multiphoton transitions. Thus for the 1 + n processes (Fig. 9), we find a broad band of efficient population transfer extending from about 40 to 60 l m. The 2 + n DMT transitions (Fig. 10) also show a considerably broadened, albeit much more orderly structured spectrum. It is also interesting to note the fairly sizable Bloch–Siegert shifts.

The conclusions are similar for the case of the 4:3 5-level system, for which results are shown in Figs. 11 and 12. Again DMT excitation spectra are characterised by broad extended peaks with partially oscillatory patterns. Thus for the 2-photon R1 ! P1 (i.e. 1 + 1) DMT transition, there is a very extended band in the k-range between 40 and 80 l m, and for the initial state R2 a typical robust feature appears around 36 l m, which corresponds to the mutual interaction of the 5-photon 2 + 1 and the 2-photon 2 + 2 DMT transitions.

As discussed further below, the broadening and splitting of these np-pulse peaks has its origin in contributions from multiphoton pump–dump transfer through the apex state, analogous to the mechanism described for the corresponding 3-level system. The pronounced 2 + 1 peak near 13 l m is entirely due to such a mechanism.

We do not explicitly show results for the 3:2 and the strongly asymmetric 30:17 case, but we note that the results in general and the trends and patterns show strong qualitative similarities with those for the other pump-to-dump ratios, except that in the 30:17 system due to the lacking simple commensurability of the R1 ! A and A ! P1 transitions the occurrence of the concomitant multiphoton pump–dump mechanism will require larger Bloch–Siegert shifts and stronger fields.

A comparison of isolated DMT with the results for the corresponding "full" system shows differences that are not very substantial, but indicate a somewhat larger degree of interference between the possible pathways than was found for the 3-level systems. Generally, weakly constructive effects seem to be present for the low-order transitions, and quenching occurs for the transitions of higher photonicity.

In order to obtain a more complete picture of DMT in the extended K-systems, in Fig. 13 we show (k, A_0)-contour plots for two selected examples, which may be considered to be representative for our systems. We observe extended and intercalated peak progressions with sizeable and closely spaced individual peaks. In comparison, for all coupling schemes (as well as for the systems not shown here) the 2 + n processes generally require higher field strengths than the 1 + n processes. This is not surprising and reflects the higher and broader barriers that have to be overcome if

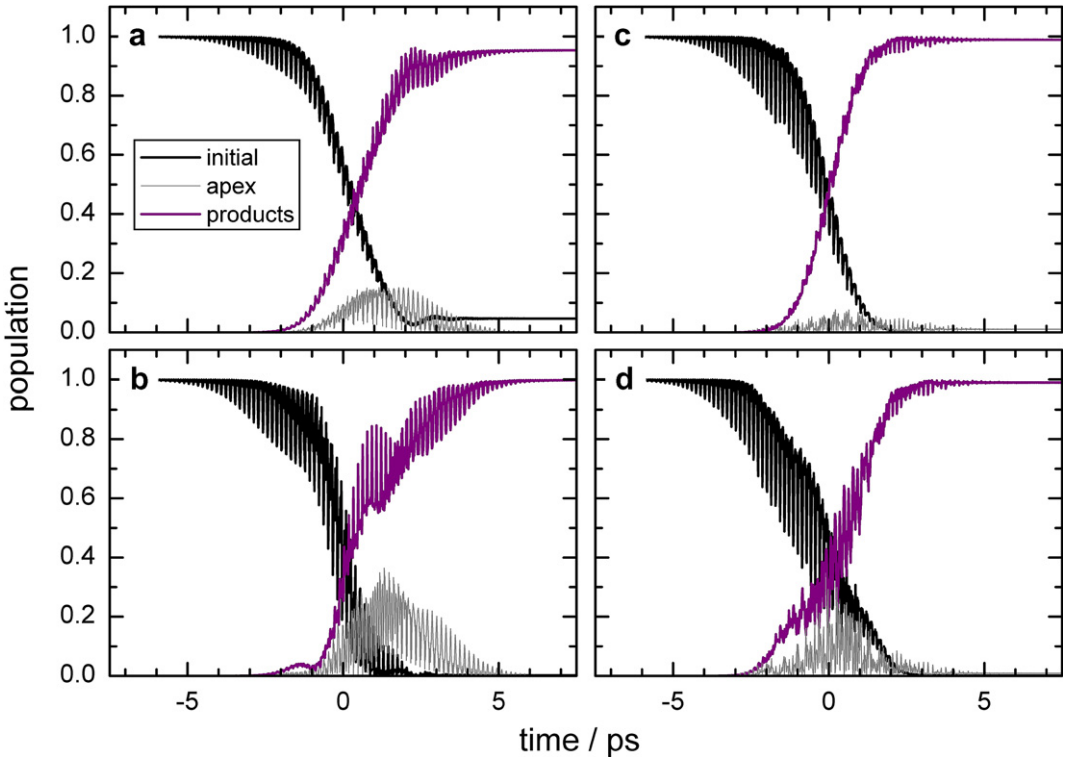

Fig. 14. DMT 2 + n population dynamics in the 4:3 5-level extended K-system. The pulse conditions for the driving laser fields marked A–D are identified in the bottom panel of Fig. 13. Bold lines starting at abscissa value 1 (online black): initial state (R1) population; bold lines starting at abscissa value 0 (online purple): total target population (P1 + P2); thin grey lines: apex state (A) population. (For interpretation of the references to colour in this figure legend, the reader is referred to the web version of this article.)

one starts from the lower state. The fact that for 2 + n transitions the transfer thresholds occur at higher field strengths indicates that a smaller degree of orientational disorder will be permissible than for 1 + n processes. The effective fields resulting from the projection onto more strongly misaligned reagents will fall below the threshold and will thus fail to drive population transfer.

Fig. 14 shows the population dynamics for the four pulse settings marked A–D in Fig. 13, which are taken at the origins of neighbouring peak progressions. In all cases DMT transfer proceeds in a Rabi-like fashion and does not show substantial apex state participation. Cases A and B belong to the 6-photon 2 + 1 transition populating P1, while C and D belong to the 2-photon 2 + 2 transition populating P2. As for the 3-level system, the simply commensurable nature of the 4:3 parameterisation allows multiphoton pump–dump processes through the apex state at the nominal frequencies of direct Rm-to-Pn transfer, which strongly couple to the DMT thus forming the extended peak structures. The extended ridges from which the pairs (A, B) and (C, D) are taken represent DMT p-pulses with different degree of pump–dump participation.

5. Dipole-mediated tunnelling isomerisation: population transfer in a dipolar 11-level extended K-system

To get an idea how DMT may act in a typical molecular situation, we use the simplistic HCN/HNC 11-level model system described in Section 2.2, which includes the main pathways of the isomerisation of highly bend-pre-excited HCN to HNC.

Our main results are collected in Figs. 15 and 16, where we show the total isomerisation probability as the sum of all HNC level populations. The initial HCN state, (0, 18, 0), is the third-highest localised J = 0 bend state in

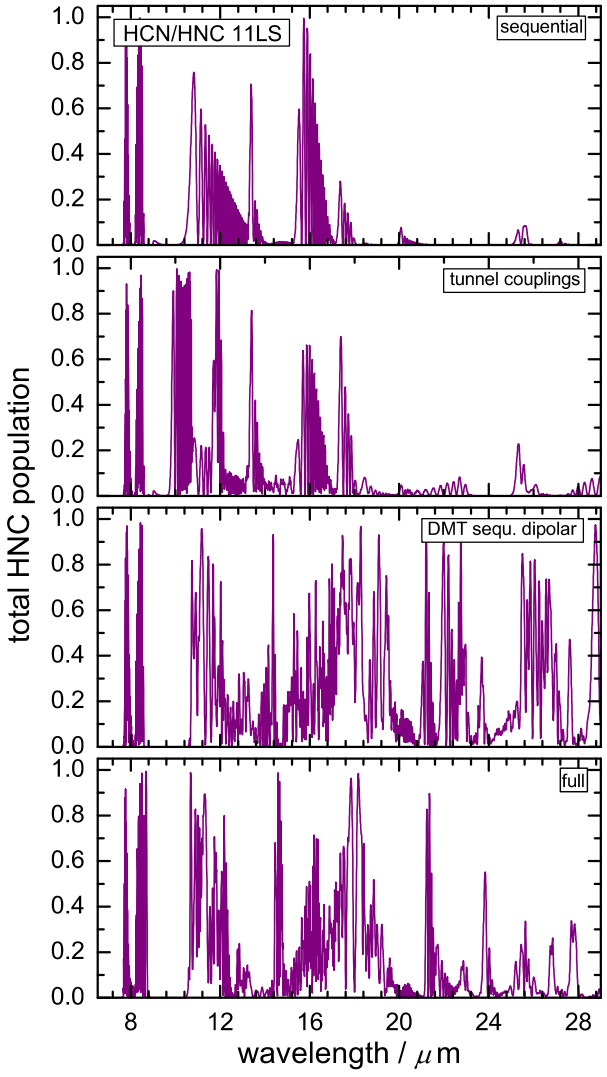

Fig. 15. Single pulse total isomerisation probability in the 11-level reduced basis HCN/HNC model system for a peak amplitude $A_0 = 0.015$ a.u. and the pre-bend excited initial HCN state (0, 18, 0). The four panels show from top to bottom the purely sequentially coupled non-polar system, the non-polar system with all tunnel couplings (but no ladder overtone couplings) added, the purely sequential dipolar system, and the fully coupled dipolar system.

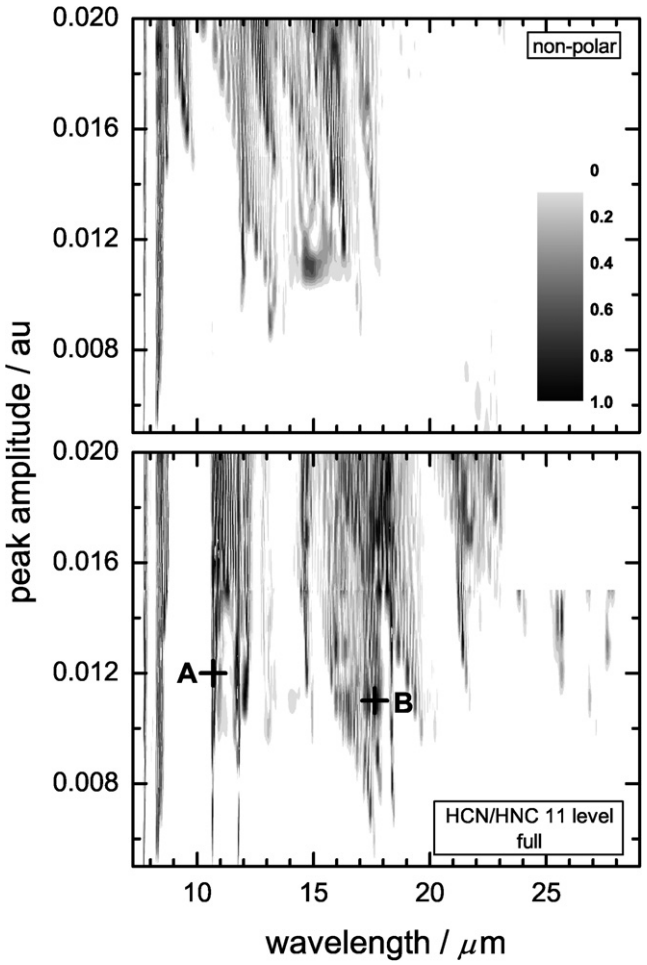

Fig. 16. Contour plots in the (k, A_0) plane for the single pulse isomerisation probability in the 11-level reduced basis HCN/HNC model system. Other conditions are as in Fig. 15. The points marked A and B in the lower panel denote conditions, for which the population dynamics are shown in Fig. 17.

the HCN well. Accordingly the transitions studied can be described as 3 + n processes. Compared to the 1 + n and 2 + n processes in the 3- and 5-level systems, we may expect a reduced efficiency of population transfer or, equivalently, a need for higher field strengths. As anticipated, the results are somewhat less spectacular than the ones for the smaller model systems. In particular, the "reactive" frequency ranges become narrower and more stratified than in the simple K-systems. Nevertheless, extended zones of reactivity are present, in particular at longer wavelengths. In detail, in Fig. 15 we show a step-by-step partitioning of the effects acting in the fully coupled 11-level system, performed for a strong field with $A_0 = 0.015$ a.u.

Due to the near 2:3 commensurate nature of the pump- and dump-frequencies, a very strong single pulse can isomerise even the sequentially coupled system without any tunnel or overtone couplings or permanent dipole moments, simply by multiphoton ladder climbing up and down through the apex state. The inclusion of direct tunnel couplings is not very effective, in fact with the dipole matrix elements as given, direct tunnelling would require longer pulses. In contrast, DMT is again a useful mechanism providing enhanced isomerisation, although it is clear that it is most efficient for long-wavelength high-photonicity transitions. Finally, in the fully coupled dipolar system isomerisation is partially quenched in comparison with DMT, indicating that interference among the multitude of possible pathways is slightly destructive in nature.

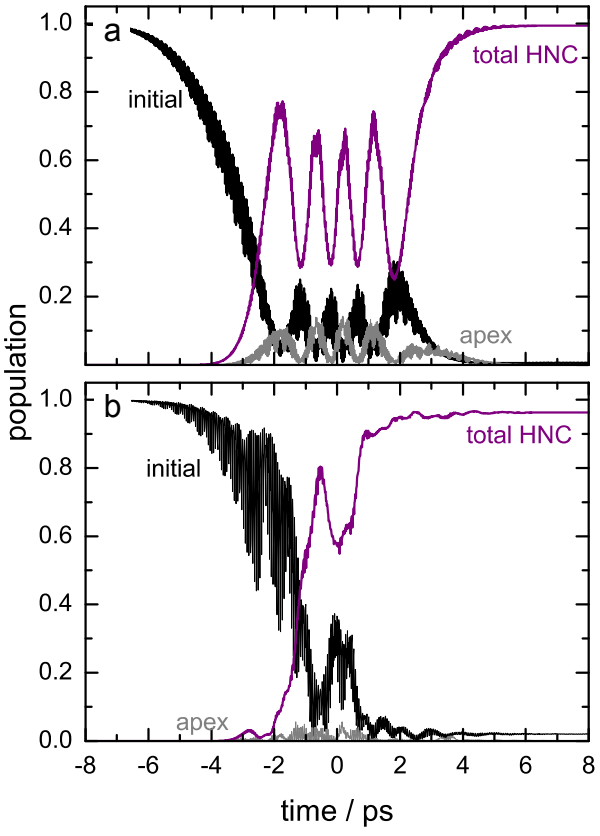

Fig. 17. Single-pulse isomerisation dynamics in the fully coupled HCN/HNC system for initial state (0, 18, 0). The conditions for the driving laser fields are identified by points A and B in the bottom panel of Fig. 16. Bold lines starting at abscissa value 1 (online black): initial state population; bold lines starting at abscissa value 0 (online purple): total HNC population; thin grey lines: apex state population. (For interpretation of the references to colour in this figure legend, the reader is referred to the web version of this article.)

Returning to the 11-level system, despite the increased complexity the isomerisation dynamics for selected pulse conditions do still indicate direct population transfer, with a well developed, only weakly perturbed Rabi-type pattern, even in the presence of full coupling. Fig. 17 shows that there is very little transitional apex state population. Both fields finally populate HNC superposition states. For A, we obtain a superposition state with 26% (0, 14, 0) and 74% (0, 18, 0), while B predominantly populates the lowest target state (0, 12, 0), carrying about 65% of the total product population, with the remaining part in (0, 20, 0). Note, however, that the final populations do not reflect the intrinsic tunnelling dynamics; by the end of HCN-to-HNC population transfer all target states are populated. The final superposition arises from the transfer of population along the adiabatic Floquet quasienergy states by the smooth tail of the driving field; in fact the transitions could be made more closely state-specific by applying a field with a longer and flatter tail.

The partial quenching in the full 11-level system noted above also leads back to the point raised in Section 2.2, namely the neglect of the split nature of the transition state of the HCN/HNC isomerisation [17]. More realistically, an extended K-system modelling the reaction should have two near-degenerate apex states (the actual splitting from the ab initio potential is 71 cm^{-1}). Correspondingly in a 12-level system taking account of this feature there is the possibility of additional parallel, competing and interfering sub-processes. Work investigating the consequences of this possibility is currently in progress.

6. Summary and conclusions

We have investigated the properties of dipole mediated tunnelling as a mechanism allowing population transfer across a barrier with a single laser pulse. By numerical simulations we have demonstrated that DMT is a mechanism that gives rise to efficient direct tunnelling transitions in simple or extended K-systems, even if there are no explicit (tunnel-) dipole matrix couplings connecting the two sides. Especially for higher multiphoton transitions, DMT turns into a robust mechanism of population transfer, operating over extended regions in wavelength (frequency) space and generating densely spaced progressions of multiple-p-pulses. Certainly for the chosen parameterisation, which is adjusted to typical molecular situations, DMT is much more efficient and robust than dipole matrix tunnel coupling or overtone coupling. Therefore, the method offers the prospect to deal with the demands of orientational disorder in molecular gas-phase samples, which for highly specific mechanisms like a pump–dump setup using reso-

nant p-pulses would be difficult to meet even for well oriented molecules.

Preliminary investigations indicate that the efficiency of the mechanism persists for larger systems, at least in certain simple configurations. In complex systems, where multiple transition pathways may be present, caution may be required in view of possible quenching caused by interference effects.

Acknowledgment

This research was supported by the Austrian Science Fund FWF within the framework of the Special Research Program F016 "ADLIS".

References

[1] M. Grifoni, P. Hänggi, Phys. Rep. 304 (1998) 229.
[2] S. Chelkowski, A.D. Bandrauk, P.B. Corkum, Phys. Rev. Lett. 65 (1990) 2355.
[3] M. Holthaus, B. Just, Phys. Rev. A 49 (1994) 1950.
[4] I.I. Rabi, Phys. Rev. 51 (1937) 652.
[5] L. Allen, J.H. Eberly, Optical Resonance and Two-Level Atoms, Wiley, New York, 1975.
[6] M.A. Kmetic, W.J. Meath, Phys. Rev. Lett. 108A (1985) 340.
[7] S. Nakai, W.J. Meath, J. Chem. Phys. 96 (1992) 4991.
[8] A. Brown, W.J. Meath, P. Tran, Phys. Rev. A 63 (2000) 013403, and references cited therein.
[9] J.H. Shirley, Phys. Rev. B 138 (1965) 979.
[10] C.A. Marx, W. Jakubetz, J. Chem. Phys. 125 (2006) 234103.
[11] J. Oreg, F.T. Hioe, J.H. Eberly, Phys. Rev. A 29 (1984) 690.
[12] U. Gaubatz, P. Rudecki, S. Schiemann, K. Bergmann, J. Chem. Phys. 92 (1990) 5363.
[13] K. Bergmann, H. Theuer, B.W. Shore, Rev. Mod. Phys. 70 (1998) 1003.
[14] N.V. Vitanov, T. Halfmann, B.W. Shore, K. Bergmann, Annu. Rev. Phys. Chem. 52 (2001) 763.
[15] M. Dohle, J. Manz, G.K. Paramonov, H. Quast, Chem. Phys. 197 (1995) 91.
[16] M.N. Kobrak, S.A. Rice, Phys. Rev. A 57 (1998) 2885.
[17] I. Vrábel, W. Jakubetz, J. Chem. Phys. 118 (2003) 7366.
[18] K. Na, C. Jung, L.E. Reichl, J. Chem. Phys. 125 (2006) 034301.
[19] T. Cheng, H. Darmawan, A. Brown, Phys. Rev. A 75 (2007) 013411.
[20] J.M. Bowman, B. Gazdy, J.A. Bentley, T.J. Lee, C.E. Dateo, J. Chem. Phys. 99 (1983) 308.
[21] W. Jakubetz, B.-L. Lan, V. Parasuk, in: M. Chergui (Ed.), Femtochemistry. Ultrafast Chemical and Physcal Processes in Molecular Systems, World Scientific, Singapore, 1996, p. 86.
[22] W. Jakubetz, B.-L. Lan, Chem. Phys. 217 (1997) 375.
[23] S. Chelkowski, A.D. Bandrauk, Chem. Phys. Lett. 229 (1995) 185.
[24] J. Gong, A. Ma, S.A. Rice, J. Chem. Phys. 122 (2005) 144311.
[25] L.V. Ke'ldysh, Sov. Phys. JETP 20 (1965) 1307.
[26] P. Dietrich, P.B. Corkum, J. Chem. Phys. 97 (1992) 3187.
[27] W.J. Meath, E.A. Power, J. Phys. B 97 (1992) 3187.
[28] B. Dick, G. Hohlneicher, J. Chem. Phys. 76 (1982) 5755.
[29] F. Bloch, A. Siegert, Phys. Rev. 57 (1940) 522.
[30] S. Leasure, K. Milfeld, R.E. Wyatt, J. Chem. Phys. 74 (1981) 6197.
[31] K. Drese, M. Holthaus, Eur. Phys. J. D 5 (1999) 119.
[32] M. Holthaus, Phys. Rev. Lett. 69 (1992) 1596.